Pedestrian Dead Reckoning Based on Frequency Self-Synchronization and Body Kinematics

Michele Basso, Matteo Galanti, Giacomo Innocenti, and Davide Miceli

***Abstract*— A novel pedestrian dead reckoning method conceived to be used with sensors freely positioned not too far from the waist level is presented. Attitude and heading reference systems already built in in nowadays inertial measurements units (IMUs) are exploited to cast the sampled data into a global reference coordinate system, where human gait analysis can be used to figure out the motion related to each single step. In particular, vertical accelerations are processed by means of a phase locked loop to detect the pace and the steps, and then the step length is computed exploiting an empirical piecewise linear relationship with the pace, while the geometrical features of the planar acceleration are used to estimate the stride heading, based on the waist kinematics. Experiments show the good results of the proposed algorithm when using both a low-cost IMU embedded in a smartphone and a more expensive stand-alone device, highlighting the method robustness with respect to the implementing hardware.**

***Index Terms*— Dead reckoning, pedestrian navigation, phase locked loops, wearable sensors.**

I. Introduction

WITH the rise of the MEMS technology (Micro Electro-Mechanical System) many low-cost integrated sensors are now available in an increasing number of personal electronic devices, including smartphones and various wearable devices. These low-power on-body sensors can be used for the continuous monitoring of the user activities, and to constantly evaluate her/his interactions with the surrounding environment. Most of these devices contain at least an Inertial Measurements Unit (IMU), which consists of an accelerometer, a gyroscope and a magnetometer. Exploiting measurements provided by the inertial sensors it is possible to create algorithms and applications able to monitor many human activities, such as sleeping, walking, running, or other sport activities, and to provide useful health information, such as the number of steps walked or the burned calories.

Pursuing a better tracking of the above activities, researchers have recently focused the attention on extending classical navigation algorithms to pedestrian activities. Although absolute positioning can still be achieved by using the Global Navigation Satellite System (GNSS), in certain environments, such as tunnels, indoor places or close to high urban buildings, this method may heavily suffer from satellite signal blockage. Moreover, the navigation performance could be limited by the reduced speeds reached by the user, that negatively affects the recognition of the motion.

In this framework, Dead Reckoning (DR) techniques can come in handy: they are advanced algorithms, based on data recorded by inertial sensors, which are able to estimate how the user advances from a known position without relying on any external infrastructure, such as GNSS, Ultra-Wide Band (UWB) or Wireless Local Area Network (WLAN) systems. Actually, the simplest approach to exploit inertial measurements is represented by Strapdown algorithms, i.e. methods based on the double integration of acceleration data [1], [2]. However, they heavily suffer from drift errors due to the limited accuracy of MEMS-based IMU sensors. Better results can be achieved when models of specific activities are taken into account, as in the case of the human gait analysis for walking or running, where the main goal typically is the Step Detection (SD) or, in addition, the Stride/Step Length Estimation (SLE) along with the Heading Estimation (HE) of each step. When such models are exploited, one can more properly refers to Pedestrian Dead Reckoning (PDR) techniques.

SD methods are the core of any PDR. They usually aim to create a pedometer from measurements provided either by the accelerometer along the vertical axis (see, e.g., [3]–[9]), or, with a different approach, by the gyroscope (see, e.g, [10]). In this regard, the most common techniques to identify the step rely on peak detection or threshold crossing (see, e.g., [6], [8], [9], [11], [12]), and flat-zone detection (see, e.g., [13]). Here, the main critical issue is the correct identification of the step number, avoiding over or under estimations due to acceleration spikes, sensor noise or imperfect tuning of the thresholds. Therefore, the typical approach exploits combinations of low-pass filtering and moving averaging to smooth the data, but this makes the method even more sensitive from its specific calibration. Usually, such techniques also rely on the correct placement of the IMU, since its position and orientation heavily affect the shape of the signal, and then the algorithm effectiveness. That is the case of the so-called Zero velocity UPdaTe algorithms (ZUPT), which are able to perform SD and SLE at once. They rely on the observation that when the foot is in contact with the ground the measured velocity and acceleration have to be equal to zero. They generally lead to very robust methods for identifying human gaits (see, e.g., [3], [14], [15]), but they are based on the assumption that the IMU is mounted nearby the foot, a very uncomfortable position for the user that usually requires also special clothing designed for this purpose.

Manuscript received September 18, 2016; accepted November 16, 2016. Date of publication November 22, 2016; date of current version December 20, 2016. The associate editor coordinating the review of this paper and approving it for publication was Prof. Bernhard Jakoby.

The authors are with the Dipartimento di Ingegneria dell'Informazione, Università degli Studi di Firenze, 50139 Firenze, Italy (e-mail: michele.basso@unifi.it; giacomo.innocenti@unifi.it).

Digital Object Identifier 10.1109/JSEN.2016.2631629

Once the step is detected, the distance travelled by the user can be possibly computed thanks to an a priori knowledge of the mean Step/Stride Length (SL) or its real-time estimation. However, SLE is a much more complicated issue, since it depends on many factors, such as the user characteristic and the walking (or running) pace. For instance, the SLE technique proposed in [16] just relies on the user height and pace, and it leads to reasonable but not accurate results. In [5], instead, it is exploited an observed quasi-linear relationship between SL and step frequency, while other popular empirical methods are based on the variance of the vertical acceleration (see [5], [17]), and on the fourth root of its peak to peak amplitude (see [18]). Besides, ZUPT algorithms represent an alternative, too. In literature, several HE approaches have been studied, but yet the problem is basically tackled with two different approaches depending on whether the orientation of the IMU sensor with respect to the direction of motion is a priori known or not. The most methods need to know the device attitude or at least its initial position. Then, they use the gyroscope and the magnetometer exploiting either the hypothesis that the user continuously points an axis of the inertial module to the forward direction, or the knowledge of its initial heading (see, e.g., [9], [11], [15], [19]). Under these assumptions, it is simple to retrieve the navigation heading, and the research has been mainly focused on combining measurements provided by magnetometer and gyroscope in order to reject magnetic disturbances (see, e.g., [20]). These are simple though effective methods, but they are also very restrictive with respect to practical applications, since the user is forced to keep the inertial module either in hand (constantly pointing at the heading), or elsewhere in the body, but making sure to rotate it solidly with the forward direction during the run or the walk, also giving information about the IMU initial orientation with respect to the user.

However, there are also a few approaches which are almost independent from the IMU actual placement. In the approaches derived from [21] the direction of motion is estimated through a Principal Component Analysis (PCA) performed on the projection of the sampled data from the original Device Coordinate System (DCS) into a chosen Global Reference Coordinate System (GRCS). This operation can be done by computing a proper rotation matrix from the estimation of the gravity vector (see, e.g., [9], [11], [21]). The PCA methods are able to catch the principal direction of the motion from the largest data variations in the horizontal acceleration, as shown in [6], [7], [9], [11], [21], [22]. However, they neglect any other secondary component, which makes them particularly sensitive to irregular steps. Moreover, a very critical issue in PCA analysis is the use of a fixed-size sliding time window necessary to have an efficient data computation. Indeed, the temporal span strongly affects the quality of the result. On the one hand, the longer is the window, the more stable are the results and the better is the estimation of the step direction. On the other hand, however, the algorithm becomes slower in detecting the changes of direction and, then, a drift is introduced during the curves due to the procedure delay. In the literature two seconds windows are commonly used when the HE is updated after each step as they represent a good compromise between accuracy and responsiveness. Larger windows negatively affect both the accuracy and the computational cost, while only shorter windows can be used when the method is applied after each new sample. In this latter case a burst in responsiveness is achieved at the cost of a particularly high computational cost, often worsened by the need of a further averaging technique similar to strapdown algorithms.

In this paper it is proposed a PDR technique where the IMU is supposed to be freely placed at the waist level, not necessarily in a symmetric position. Good choices are, for instance, inside a pocket, hanging from the belt, fixed at the hip, kept on the belly, hung from the belt, or around the kidneys. These are very intuitive and comfortable places in which a user can wear a sensor, and, indeed, the most of male people carry the phone there, as shown in [23]. The chosen position level derives from the used kinematics analysis of the legs and lower torso accelerations, which feature a characteristic drift and oscillation, but in principle this PDR method is expected to work well even with foot and upper torso positions just with little adjustments, though it has not yet been tested there. However, a similar analysis could also be carried out for other positions, such as the wrist or the arm. The waist level and the free attitude of the sensor are particularly suitable for objects which are used also for other purposes, such as smartphones, pocket purses or fanny bags. As for possible applications of such wearable PDR devices, nowadays the user's activity monitoring is very popular, both for fitness and health purposes, but indoor and enhanced-GNSS reckoning are receiving quite the interest too [7], [9]. However, the actual implementation of the method for one of these objectives is out of the scope of this paper.

The proposed approach is based on a new SD method, which exploits a Phase Locked Loop (PLL) system. Not only this method provides accurate results even in the case of a very noisy acceleration signal, but it also represents a very flexible solution able to work at very different paces, and its computational burden just equals that of a low-pass filter. The proposed PDR method also introduces an other innovative HE. As in the PCA approach, after a change of the reference frame from the DCS to a GRCS, the horizontal plane accelerations are used to infer the direction of each step. However, while in the PCA methods only the principal component of the horizontal motion is extracted and some a priori information is often required to reduce the calibration errors due to the trade-off inherent the sliding window length (see, e.g., the experimental set ups in [9] and [11]), the proposed approach only exploits the geometrical features of the horizontal acceleration to figure out the related kinematic features of the motion. This turns out such an effective and robust approach that no additional assumptions on the IMU orientation or about the initial set up are necessary.

The paper is organized as follows. In Section II human gait analysis will be introduced from a signal processing perspective. The importance of the IMU placement will be highlighted, and this work idea about making the analysis independent from it will be discussed as well. Then, the methods for detecting the motion and the steps, and eventually for estimating the stride length will be illustrated. Section III will be devoted to describe the original technique to estimate the motion direction, while in Section IV the results of several experiments aimed to validate the proposed Pedestrian Dead Reckoning will be presented. Some final remarks in Section V will end the paper.

II. Human Gait Analysis

The use of inertial sensors for the detection and analysis of human motion has been widely studied in the past years. The first issue connected to the gait analysis is the motion detection, since during any walk the user can stop-by for many reasons. Moreover, during her/his motion, the user can also switch from walking to running, and viceversa. Therefore, before everything else, it is essential to define an automatic procedure to recognize both if the user is moving and possibly if it is walking, running, or any other meaningful activity. A popular approach consists in multi-mode detection via expert algorithms capable of discerning among several cases (see e.g. [6], [8]). However, after that all the other problems concerning SD, SLE, and HE have still to be solved. In the following an innovative PDR method, featuring an original pedometer and a new technique for estimating the motion direction on the base of human kinematics, is developed. It is based on novel and robust procedures for SD and HE, and it uses an efficient implementation of the piece-wise linear calibration approach to provide SLE. Moreover, it turns out fairly independent from the IMU placement and orientation.

A. IMU Placement

The accelerations measured by the IMU strictly depend on the sensors placement and their orientation with respect to the human body. In general, there are settings of the IMU that provide some advantages but usually they turn out very uncomfortable positions, especially for every day life. Sometimes to lessen these constraints an expert algorithm is designed to detect the current mode in the IMU positioning, but at the expense of a great increase in the complexity and the computational burden (see, e.g., [6], [8]).

In this paper, in order to achieve a fair independence from the IMU actual placement and attitude, the rotation matrix approach first presented in [21] is considered. However, with respect to the original procedure we abandon the PCA technique, because of its drawbacks. The PCA technique is then substituted with a novel method based on the kinematics analysis of the horizontal plane accelerations. Notably, such a method is definitely not computationally intensive, since the HE is provided only at the end of each step, and the procedure's complexity turns out similar to that of an elementary low pass filter. In particular, it works in combination with the SD algorithm proposed hereafter and it uses all the acceleration data belonging to the last step to derive information about the starting and the finishing point of the waist motion. Indeed, the kinematics studied so far requires that the IMU is placed not too far from the waist, while no specific constraints are imposed to the IMU orientation. Therefore, the only assumption needed by this paper's approach is that the IMU has to be located in the lower-torso/upper-leg area, not necessarily in a symmetric position though. Hence, the assumption about the IMU placement is definitely not an actual limitation. However, future developments will aim to widen the kinematics analysis to other useful IMU positions, such as the wrist used by smartwatches.

In the following framework the IMU orientation is set free, because the IMU itself is supposed to be provided with a built-in Attitude and Heading Reference System (AHRS) algorithm that allows one to project the sampled data from the DCS to a GRCS. It is worth stressing that this is a common scenario for recent smartphone IMUs. The AHRS algorithms are able to real-time estimate the IMU attitude with respect to a fixed reference frame in terms of the Euler angles φ, ϑ and ψ or, equally, by means of the unit quaternion (see, e.g., [24]). There are many possible GRCS, but in the following the North-East-Down (NED) frame has been chosen. According to standard notation the NED frame will be referred to as an xyz euclidean space, where the axes x, y lie on the horizontal plane and they are orientated respectively toward North and East, while axis z points the vertical direction. Once that the attitude of the IMU is known, it is possible to define the rotation matrix $R_{\text{BODY}}^{\text{NED}}$ from the DCS to the GRCS. This rotation matrix can be used to cast the measurements, provided by the sensors and referred to the device frame, into the fixed NED frame, thus decoupling them from the IMU orientation. Hereafter, all the measurements will be directly referred to the NED frame.

B. Motion Detection

The experiments, performed to develop the motion detection, show that an index useful to distinguish between motion and arrest is the standard deviation of the vertical acceleration a_z computed on the values acquired in the last two seconds. If t is the actual clock value, the set of the sampling times t_k over the last two seconds can be conveniently denoted as $\Phi_2(t) = \{t_k : t_k \geq t - 2\}$, and its cardinality $n_2(t)$ provides the number of samples in the same time window. Denoting also the vertical acceleration sample at t_k as $a_z(t_k)$, the above standard deviation is given by

$$\sigma_z(t) = \sqrt{\frac{1}{n_2(t)} \sum_{t_k \in \Phi_2(t)} (a_z(t_k) - \mu_z(t))^2} ,$$

where

$$\mu_z(t) = \frac{1}{n_2(t)} \sum_{t_k \in \Phi_2(t)} a_z(t_k) .$$

Notably, both $\sigma_z(t)$ and $\mu_z(t)$ can be efficiently computed by saving t_k and $a_z(t_k)$ in two time-regulated buffers (so to contain only samples in the desired time frame), and updating the sums with the pushed in and pulled out samples.

It is worth underlining that a_z provides information about the state of motion independently from the walking pace. In particular, if the walking pace increases, the amplitude of the vertical acceleration and, consequently, the standard deviation increases as well. Therefore, in order to identify the motion it is sufficient to use a proper threshold, because even at a very low walking pace the vertical acceleration

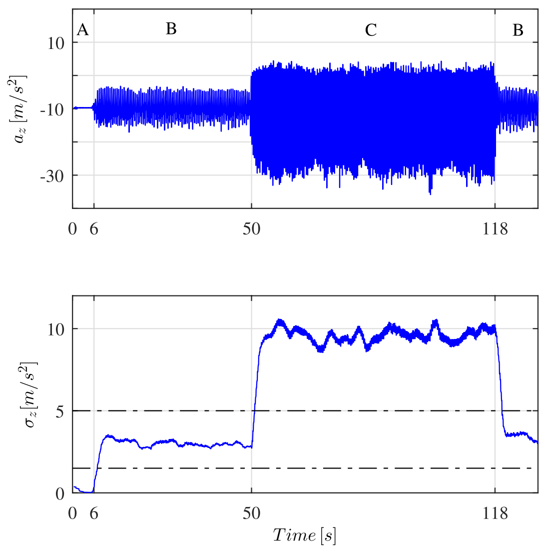

Fig. 1. Experimental results of the motion detection method. Top: vertical acceleration a_z during stop (A), walking (B) and running (C) activities. Bottom: standard deviation computed on a sliding window and the two thresholds (dash-dotted lines) employed to detect the type of motion.

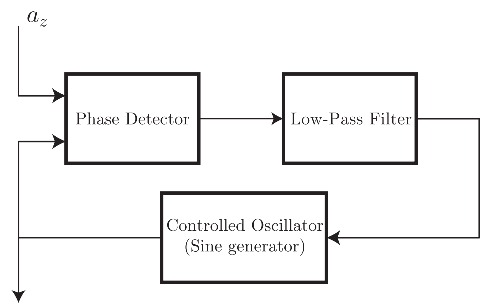

Fig. 2. The Phase Detector produces a signal whose main component is related to the phase difference among the original signal and the sine wave generated by the Controlled Oscillator. The Low-Pass filter isolates this value, that is then used to vary the phase of the CO accordingly.

has a significant amplitude compared to its high-frequency fluctuations.

In the proposed algorithm the threshold on a_z has been empirically chosen equal to 1.5 m/s^2. When an arrest is identified, i.e. when the standard deviation falls below that threshold, the SD method is disabled. In such a way the algorithm computes neither the heading nor the step length as long as the standard deviation is below the threshold. The SD procedure is immediately enabled when the standard deviation exceeds the threshold again, and this instant is saved to properly compute the step period without considering the arrest time. In order to distinguish between walking and running activities, a_z can be exploited again just by using an additional threshold at 5 m/s^2. Indeed, during running, the amplitude of the vertical acceleration is definitely greater with respect to the walking case. Consequently, the standard deviation of a_z undergoes significant changes during the transient between walking and running, turning out a very good index to discern the type of motion. It is worth underling that the standard deviation of the vertical acceleration is mostly related to the pace of the activity. Thus, the two thresholds previously described correctly work with every user, both female and male, independently from the features of her/his body. Figure 1 shows the standard deviation of the vertical acceleration during a mixed test composed of initial standing, walking, running and changes in running pace.

C. Step Detection

The proposed SD method relies on the inertial data acquired by the IMU sensors, but to detect the step only a_z is actually necessary, since it provides sufficient information about the phases of the gait cycle. Again, it is worth underlining that the original accelerometer data are first cast into the NED fixed frame by using for example the Euler angles provided by an AHRS system, as previously mentioned. This transformation is necessary to distinguish the accelerations along the vertical axis z from those on the horizontal xy plane.

The main idea of the proposed procedure is to identify the start and the end of each single step in correspondence of the maximum peaks of the vertical acceleration. In such a way the SD method turns out independent from the velocity of walking/running. However, the raw data provided by the accelerometer are very noisy, thus the raw vertical acceleration can not be used to separate the different steps because of the many spurious peaks. These unwanted peaks can be removed with a low pass filter with an appropriate cut-off frequency which removes the harmonic associated with frequencies higher than the step frequency. Nevertheless, such a solution is difficult to implement, since the appropriate cut-off frequency is not constant, but it is connected to the step frequency. In order to remove the noise, maintain the informative signal, and to achieve solid results, it would be necessary to introduce a complex low-pass filter with a time-varying cut off frequency depending on the pace. Nonetheless, this fixed cut-off frequency plus proper threshold has recently become popular (see, e.g., [6], [7]), because of its simple implementation. However, the experiments reported in the same literature confirm the critical issues previously commented and the difficulties in calibrating the right threshold.

To overcome the above tuning problems, a novel, more efficient and more flexible solution, able to improve the robustness of the SD method, has been developed by using a PLL based approach [25]. A common PLL consists of a Controlled Oscillator (CO), a phase detector, a low-pass filter, interconnected as in Figure 2, and it can be realized both via software and via low-cost electronics. The PLL can be regarded as a control system that generates a sinusoidal output signal, whose frequency and phase tend to match those of its input signal. Here, the PLL is used to synchronize its output with the input acceleration signal a_z. The phase detector compares the phases of a_z and of the periodic signal generated by the CO, and then it adjusts the oscillator to keep them matched through a filtered feedback loop. Keeping the input and output phases locked implies having locked also the frequencies. Consequently, in addition to synchronizing the signals, a PLL is able to track the input frequency. In the proposed application the PLL is used to extract a sine wave

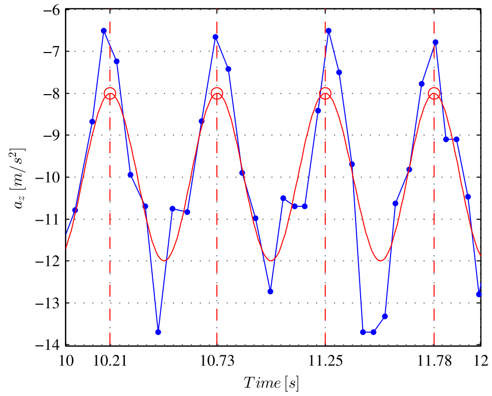

Fig. 3. Vertical raw acceleration a_z (blue) and the output of the Phase-Locked Loop system (red), properly scaled and vertically shifted to be compared to a_z. Vertical dashed lines indicate step detection (SD).

synchronized with the fundamental frequency of the vertical acceleration, in order to remove all the spurious peaks that could compromise the SD. As shown in Figure 3 the PLL can lock the raw acceleration data a_z. To guarantee that the PLL locks the input signal, a free-running frequency possibly close to the real one has to be chosen. However, this is not restrictive, because during walking or running the step frequency can vary with small absolute changes, lower than $1Hz$. Therefore, it is sufficient to set a free-running frequency in the middle of the possible range of variation to allow the PLL to lock the vertical acceleration. For example, regarding just the walking activity a free-running frequency of $1.8\ Hz$ guarantees fast locking. Once that the PLL output is available, the start and the end of every single step can be detected just by finding the peaks of the PLL output, as shown in Figure 3. Experiments show that such a step detection method also provides an extremely accurate evaluation of the step frequency as a by-product. Indeed, if the start and the end of the k-th step are known, the period T_k of the step is the elapsed time between them, and the instantaneous step frequency can be computed as $f_k = 1/T_k$ without recurring to spectral analysis.

D. Step Length Estimation

For the complete characterization of the human gait, the correct estimation of SL is necessary, as well. Even though a constant value approximation of SL would be quite simple to realize, the problem becomes very complex when an estimation closer to the actual value is required, since both personal features of the subject and environmental conditions shaping the stride have to be considered. The step length changes from one person to another, and even the same person modifies her/his own SL as the speed changes and in presence of obstacles. A basic factor for the determination of SL is the height of the user. It is generally true that taller people make longer steps, and for this reason they can cover longer distances with the same number of steps. Anyhow, it is necessary to observe that these physical and geometric argumentations are not absolute rules. Personal features or styles are often more important than these considerations. Even if the average SL of a single person usually remains almost constant, each single step contains a correction of few centimetres, which has to be considered and evaluated in order to achieve the closest estimation to reality. This is a crucial point in the long run, when the accumulating error can be a limit for the accuracy of the PDR system.

A good estimation of SL can be achieved taking into account the personal features of the user, the step frequency, and the slope of the road. There is definitely a strong connection between step length and frequency. In particular, it has been observed that within a certain interval of frequencies the SL dependence from the step frequency is almost linear, as shown in [5]. Hence, quantitatively computing such linear law turns out almost equivalent to figure out some of the user features affecting SL. This procedure can be carried out by repeated calibration tests, performed using different walking speeds. The experiments should be done along straight paths with a known length, and in a single test the subject should try to maintain the same pace of stride. In such a way the experimental data can be used to determine both the average frequency and the corresponding average SL. Given that both the steps number N and their frequencies f_k, $k = 1, \cdots, N$, directly derive from the SD method as previously mentioned, the average frequency $\bar{f}$ can be computed as

$$\bar{f} = \left(\frac{1}{N} \sum_{k=1}^{N} \frac{1}{f_k} \right)^{-1}. \tag{1}$$

Moreover, from N and the total distance D covered in each experiment, the average step length can be computed as

$$\overline{SL} = \frac{D}{N}. \tag{2}$$

Since each experiment provides data which are sufficient only to determine the correspondence between the average frequency $\bar{f}$ and the average step length SL, every subject should repeat this test as many times as possible, trying to vary the speed each time. Eventually, in the graph of the average frequency versus the average SL each experiment provides a single point. The set of all these points, i.e. $P_i = (\bar{f}_i, \overline{SL}_i)$, $i = 1, \ldots, M$, where M is the number of experiments, can be used to compute the best linear approximation, for instance via the least squares method. In a mobile app perspective, these tests can be regarded as the initial calibration of the device. Moreover, it is worth noticing that in a smartphone scenario the need of the exact distance covered during each test is not an actual limitation, since these devices are usually provided with many absolute positioning systems, such as the GNSS. In this regard, the longer the path, the more accurate the results.

Several tests have been carried out on different subjects, both males and females, and the linear dependence between these two quantities was confirmed. It is worth stressing that the linear approximation of their mutual dependence turns out good only on limited interval of human characteristic stride frequencies, usually within $[1.5 \div 2.2]\ Hz$ concerning the walking and $[2.7 \div 4.2]\ Hz$ for the running. It has empirically been shown that between different subjects there may be big differences. Indeed, not only the best interpolating straight line changes, but also the interval in which this approximation can be considered acceptable varies, as well. Figure 4 shows

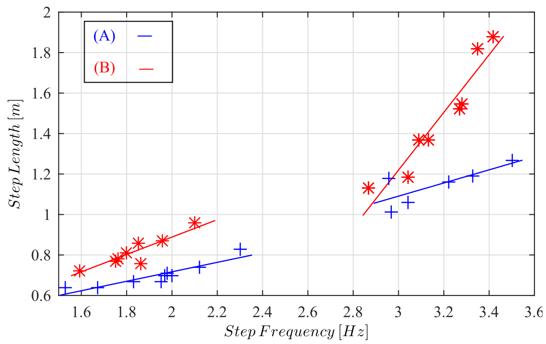

Fig. 4. Results of the step length calibration tests for walking (left region) and running (right region) for two different persons: (A) is a male user 1.68 m, 61 kg (blue '+' marks), whereas (B) is a male user 1.93 m, 105 kg (red '*' marks). The blue and the red lines are the best linear approximations given by least square theory.

an example of calibration test. Observe that, in general, the calibration test must be carried out both for walking and running. Therefore, a global description of the dependence of SL from step frequency has the form of a piece-wise linear function.

III. Heading Estimation

This work pursues a procedure for heading estimation with the following features:

- *low cost*, i.e, able to use IMUs commonly integrated in smartphones and wearable devices, not requiring the installation of specific infrastructures (e.g., a wifi network);
- *automatic*, i.e., free from constraints about the position and the orientation of the device, increasing the commercial potential;
- *suitable for both indoor and outdoor applications*, i.e., not based on any assumption about the application environment.

In order to satisfy the above properties, the HE algorithm developed hereafter has been based on the idea (shared with PCA method, see also [21]) that, if the orientation of the IMU can be estimated with respect to a GRCS, then the related accelerations in the fixed frame can be used to detect the direction of motion independently from positioning of the IMU. This approach relies on proper rotation matrices computed via AHRS algorithms, which definitely increase the complexity of the algorithm, since the computation of the rotation matrix is a quite complicated problem by itself (see, e.g., [11]). However, this can not be considered an actual constraint, thanks to the increasing computational power of smartphones and wearable devices, and to the constantly increasing integration of built-in AHRS algorithms even in low cost IMUs. The proposed HE method, indeed, exploits AHRS functions to transform the accelerations from the DCS to the NED fixed GRCS, thus becoming a method completely transparent to the user, since the IMU positioning can be done everywhere close enough to the waist area, as already mentioned.

On these premises the algorithm has been originally developed by exploiting the phases of pedestrian motion and their relationship with the acquired data, i.e. the method has been conceived to directly exploit the gait analysis and in particular the body dynamics around the waist level.

In the proposed approach the HE is performed on each detected step and only the accelerations on the xy plane are actually used to recognize the motion direction, that is represented by the angle θ with respect to the x axis. However, this assumption is not restrictive, because, even if the motion occurs uphill or downhill, the accelerations on the xy plan are predominant in comparison with the ones along the z axis during a sloping path. The accelerations measured in the DCS and transformed into the fixed GRCS are due to the motion along the forward direction and the maintenance of balance. The former are accelerations useful to identify the heading, while the latter can be regarded as noise, and they depend on the average of the forward velocity, the type of activity, and the surface on which the motion occurs. During a particularly slow walking pace or when avoiding an obstacle, for example, it is legitimate to expect lateral accelerations comparable with the accelerations in the forward direction, but with the increase of the walking pace the lateral acceleration usually becomes more and more negligible with respect to the longitudinal one. In general, the assumption that lateral accelerations are negligible with respect to forward accelerations is too strong, because the human body does not proceed exactly on a straight line, but it naturally oscillates around the average direction. This is a critical issue in PCA methods, which are unable to provide stable results during these "irregular" steps that feature comparable forward and later accelerations. In PCA techniques the stability of the results is crucial for the final accuracy of the HE, but unfortunately, just when forward and lateral accelerations are comparable, PCA needs a longer sliding window of data to stabilize the estimate, with a consistent loss of responsiveness and the introduction of undesired drifts. Such a problem may be approached by applying PCA after each new sample using shorter windows, and then smoothing the result, but this will largely increase the computational cost. Our method, instead, not only lessen the computational burden by computing the heading only at the end of the step, but each estimation requires only basic computations. Notably, the method exploits both the forward and lateral acceleration to infer the features of the related stride, from which it derives the step direction of motion.

The proposed HE method can be explained by recurring to the graphical representation of the accelerations a_x and a_y on the plane xy during a left-right step window, after the signal has been smoothed by removing all the frequencies above that of the single step by means of a low-pass filtering with proper cut-off frequency. Figure 5 shows that during each step such smoothed planar accelerations describe a pseudo-elliptical shape on the xy plane as a mix of forward and lateral accelerations, the principal axis being related to the forward motion. Intra-step accelerations due to sudden movements related with balancing or obstacle avoidance introduce high frequency distortions in the basic elliptical shape. If their magnitude is sufficiently small, the basic shape can still be recognized, but, when they grow bigger than the forward acceleration, the main direction featured by the curve may deviate from the actual heading of the user. Figure 6 shows

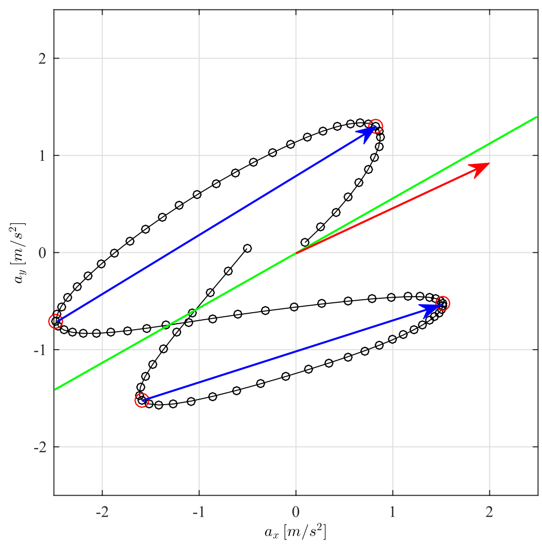

Fig. 5. Representation of a_x and a_y on the horizontal plane during a sequence of left and right steps. The signal has been smoothed by filtering all the frequencies above $2.3Hz$. The red circles represent the tip and the tail of the ellipses, whereas the blue arrows represent the tip-to-tail vectors. Ground-truth is indicated by the green line, while the red arrow is the HE averaged over the two steps.

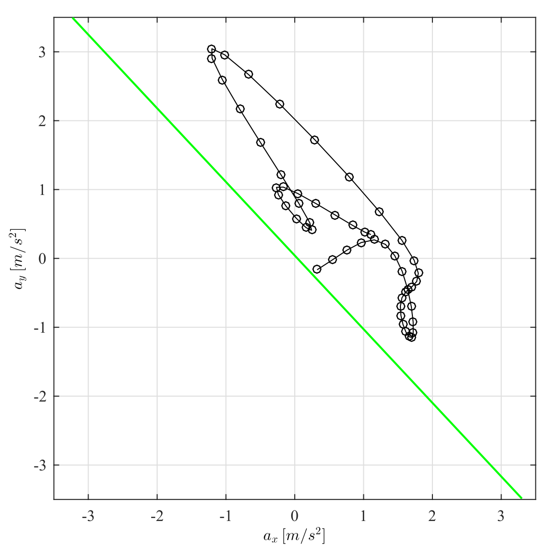

Fig. 6. Raw planar accelerations a_x and a_y related to an irregular step. The distortion does not hide the existence of a main direction of the motion which is aligned to ground-truth (green line).

the curve of the raw planar acceleration corresponding to an irregular step.

According to the above reasoning, we suggest to estimate the direction of the user by recovering the underlying elliptical shape in the planar acceleration data. Indeed, if a single step as identified by the SD method is not excessively irregular, it can be reduced in the plane xy to a pseudo-ellipse, whose "tip" and "tail" represent the starting forward acceleration followed by the related deceleration direction, respectively. Their connecting vector is the closest to the actual motion followed by the waist during the stride. It is worth observing that each tip-to-tail vector has the tip on the acceleration phase, so it is possible to identify the direction of motion in addition to the line of action [7]. PCA techniques, instead, need to combine the planar acceleration with the vertical one to discern the actual moving direction along the line of action. Figure 5 shows the tip-to-tail vectors (in blue) associated to two consecutive ellipses. An important advantage of this geometrical approach is its flexibility, since it works well with both walking and running, along both straight and curve paths, and eventually because even the irregular steps features a tip-to-tail characteristic. Many experiments have clearly shown that each pseudo-ellipse is rarely headed towards the real direction of motion, but it points to a direction that is slightly shifted to the right or to the left depending on the step which it is referred to. In particular, during the right step the ellipse points towards a direction shifted to the right, and vice versa during the left step. This is an effect due to the periodical rotations of the lower torso around the real direction of motion during a walk or run, and it can be reduced just by averaging the tip-to-tail vector directions of two consecutive steps, so defining the average heading estimation (A-HE) shown in Figure 5 by the red vector.

The underlying pseudo-ellipses associated to a stride (i.e., a double step sequence) can be obtained as in Figure 5 by smoothing the raw data through a proper cut-off frequency. Empirical observations suggest that, if the elliptical shape is preserved, the tip and tail can then be computed by looking for the local maxima in the planar acceleration magnitude as shown in Figure 7. However, such an approach would lack of flexibility and robustness, since no other local maxima must be present, i.e. the frequency has to be perfectly chosen. Moreover, in general the right cut-off value varies in time due to the pace, and also it could be different for every user. Therefore, we exploit Fourier theory to extract just the first and the second harmonic components over two consecutive steps, so that the magnitude of the approximating signal has exactly two local maxima for every step. In particular, let us define t_k as the end of the k-th step, being $T_k = t_k - t_{k-2}$ the period of the related stride. Then, we approximate the planar acceleration vector $a_{xy}(t)$ in (t_k, t_{k-1}) by its second order Fourier series removed of the continuous component and computed over the last stride, i.e. over the interval (t_{k-2}, t_k)

$$a_{xy}^{(2)}(t) = \sum_{n=1}^{2}\left[\alpha_n \cos\left(\frac{2\pi}{T_k}nt\right) + \beta_n \sin\left(\frac{2\pi}{T_k}nt\right)\right] \quad \forall t \in (t_{k-1}, t_k),$$

where the coefficients α_n and β_n are computed as follows:

$$\alpha_n = \frac{2}{T_k}\int_{t_{k-2}}^{t_k} a_{xy}(t)\cos\left(\frac{2\pi}{T_k}nt\right)dt,$$
$$\beta_n = \frac{2}{T_k}\int_{t_{k-2}}^{t_k} a_{xy}(t)\sin\left(\frac{2\pi}{T_k}nt\right)dt.$$

Figure 7 shows the magnitude of the filtered planar acceleration against the unbiased second order Fourier approximation $|a_{xy}^{(2)}|$ over two consecutive steps, while Figure 8 provides a comparison of the corresponding acceleration signals directly on the xy plane. The comparison between the smoothed method and the second order Fourier approach in the computed

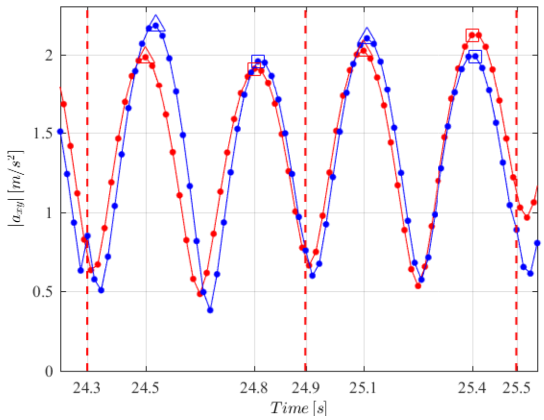

Fig. 7. The magnitude of the filtered planar acceleration signal $|a_{xy}|$ over two consecutive steps (blue) is compared with the amplitude of the unbiased second order Fourier approximation (red). The end of each step is shown by the vertical dashed lines. Within each step interval, the triangle and the square marks (on the local maxima) define the values of t_{tip} and t_{tail}, respectively.

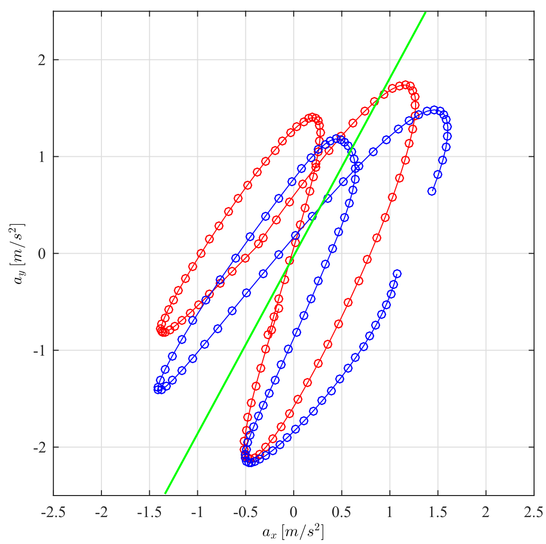

Fig. 8. The unbiased Fourier approximations of the planar accelerations (red) are compared on the xy plane with the signals a_x and a_y smoothed with an exact cut-off frequency (blue). The green line shows the direction of ground-truth.

A-HE is also reported in Figure 9: during an experiment of about 100 steps the differences amount at most to few degrees.

Summing up, the A-HE method can be described according to Algorithm 1.

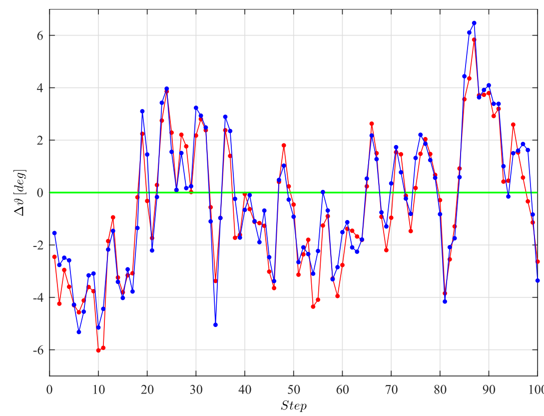

Fig. 9. The A-HE (relative to ground-truth) obtained by the smoothing method (blue) and by the unbiased second order Fourier approximation (red) are compared in an experiment featuring several steps.

Algorithm 1 Set of Operations for Computing the Average Heading Estimation (A-HE)

1) `Detect each single step (e.g. by means of the PLL-based procedure);`
2) `at the end` t_k `of each step:`
   a) `compute the unbiased second order Fourier approximation of the planar acceleration;`
   b) `calculate the magnitude signal of the Fourier approximation onto the horizontal plane;`
   c) `find the two peaks in that magnitude that correspond to the acceleration and deceleration pair associated with the step;`
   d) `calculate the tip-to-tail vector components along` x `and` y `axes`

$$\Delta a_x = a_x(t_{tip}) - a_x(t_{tail}) \ ;$$
$$\Delta a_y = a_y(t_{tip}) - a_y(t_{tail}) \ ;$$

   `and the vector direction`

$$\vartheta_k = \operatorname{atan2}(\Delta a_y, \Delta a_x) \ ;$$

   e) `estimate the heading (A-HE) by averaging the last two directions` ϑ_k `and` ϑ_{k-1}.

IV. Pedestrian Dead Reckoning

The procedures illustrated in Sections II and III have been combined to implement a complete PDR system. The resulting algorithm has been validated by using data collected either from a *common smartphone* and from a more *expensive stand-alone IMU*.

The smartphone IMU comprises the following MEMS sensors:

- a capacitive MEMS triaxial accelerometer produced by STMicroelectronics (LSM330DLC);
- a MEMS triaxial gyroscope produced by STMicroelectronics (LSM330DLC);
- a piezoresistive MEMS pressure sensor produced by STMicroelectronics (LPS331AP);
- a triaxial magnetometer produced by Asahi Kasei Microdevices Corporation (AK8975).

These sensors provide direct measurements of the accelerations, the angular velocities, and the magnetic field along three axes. Moreover, the IMU indirectly provides the smartphone attitude and orientation thanks to its built-in AHRS algorithm (*iNEMO Engine Software* [26]). This implements a sensor fusion and filtering algorithm that uses advanced procedures to integrate outputs from multiple MEMS sensors.

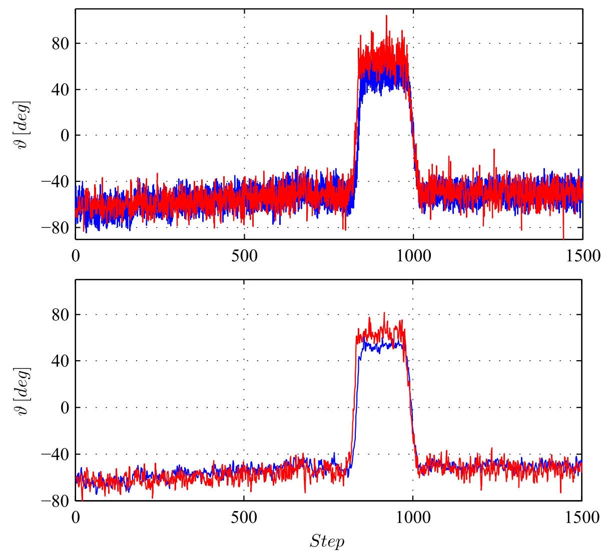

Fig. 10. Top: comparison of the HE by single step obtained via the stand-alone (blue) and smartphone (red) IMUs during the same experiment. Bottom: comparison over the two-step-averaged heading estimations A-HE.

The stand-alone IMU used in this work is the MTi-G produced by Xsens Technologies BV [27]. It comprises a triaxial accelerometer, a triaxial gyroscope, a triaxial magnetometer, a static pressure sensor, a temperature sensor, and a GPS receiver. The IMU includes also an AHRS algorithm to provide the IMU orientation.

All the presented tests have been performed using the same sampling rate ($50Hz$) to collect data from the IMUs, although the proposed method is still reliable with sampling rates as low as $15Hz$. Notably, the application of the proposed heading estimation algorithm employing such different devices provided very similar results. In Figure 10 a comparison in the use of the smartphone and the Xsense MTi-G IMU is reported for a long walk of about 1500 steps showing differences in heading estimation that remain within 5-6 degrees. Since other tests have confirmed the above result, we conclude that the IMU choice is not critical in this respect since the HE algorithm is pretty robust to raw data noise.

A. Experimental Results

Many experiments have been carried out in order to validate the proposed HE and PDR algorithms. In these tests the initial position of the user is known to the observer, but such an information is hidden to the algorithm, that, therefore, provides estimates of angles and distances relative to the initial condition. Moreover, the IMU is worn either on the belt or in a pocket. For the sake of a clearer evaluation of the error in the estimations of direction and position, the testing paths followed by the user have been previously defined on a reference map. Hence, the real direction and distance of the motion are known and will be hereafter referred to as ground-truth. Besides, in the following experiments the focus is just on validating the proposed approach to PDR, and so the actual algorithms implementation as well as the related software optimization will not be considered.

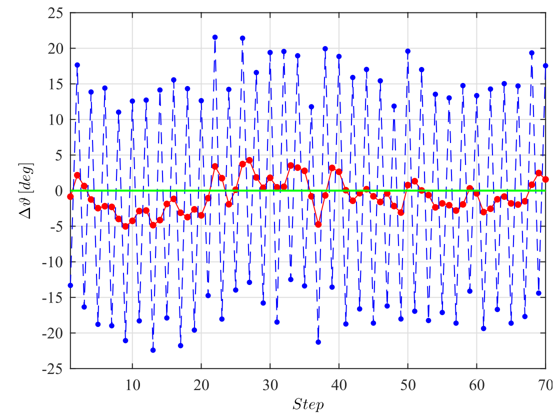

Fig. 11. Heading estimation (relative to ground-truth) computed for the single step (blue), and considering the average value computed over the last two steps (red) during a walking in straight line.

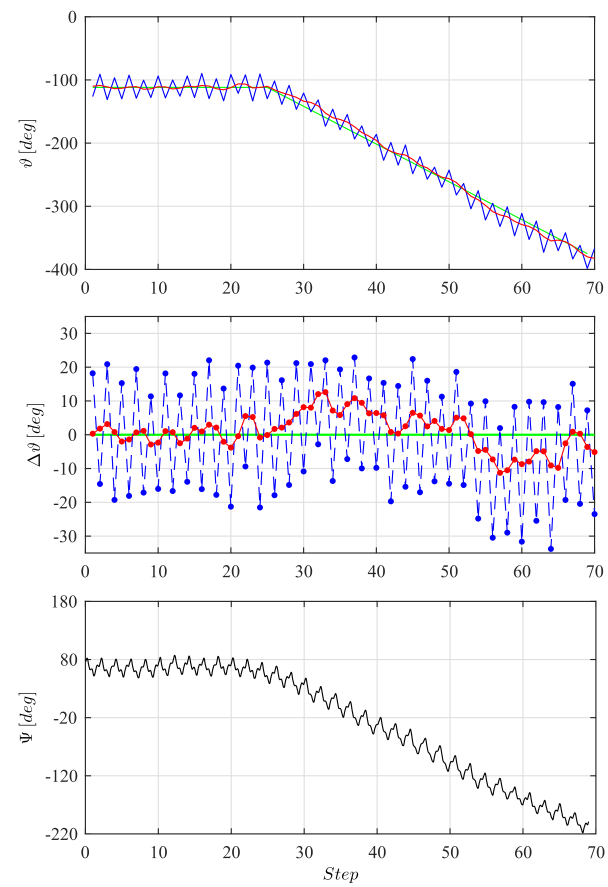

Fig. 12. Experimental results of a test carried out on a circular path. Top: ground-truth (green), estimated direction of motion (blue), and average value computed on the last two estimated directions (red). Center: differences wrt ground-truth. Bottom: heading of the sensor device provided by the gyro. For the sake of simplicity the device attitude was never changed during the test.

Figure 11 shows the estimated direction of motion in a test in which the user walks following a straight line. As previously observed the single-step HE (blue) oscillates around ground-truth (green) due to the waist rotation. The two-step-averaged A-HE attenuates these fluctuations and guarantees a more accurate estimation of the direction of motion.

Figure 12 shows the experimental results of a test where the user at first follows a straight line and then a circular path.

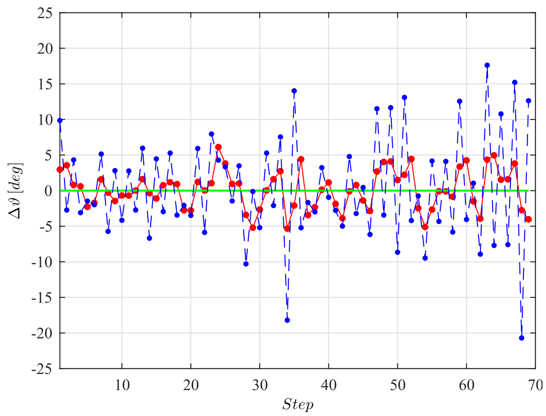

Fig. 13. Direction of motion (relative to ground-truth) for the HE (blue) and A-HE (red) algorithms during a running in straight line.

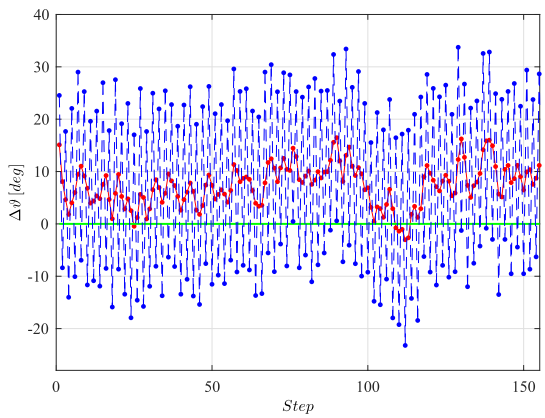

Fig. 14. Direction of motion (relative to ground-truth) for the HE (blue) and A-HE (red) algorithms during a walking on a straight line under magnetic disturbance.

TABLE I

ACCURACY RESULTS FOR THE PROPOSED PDR SYSTEM ON A NUMBER OF OUTDOOR PATHS OF DIFFERENT LENGTH, WALKED (W) OR RUN (R) BY TWO DIFFERENT TESTERS (USER A AND B ARE DESCRIBED IN FIGURE 4). THE MAP OF TEST # 3 IS REPORTED IN FIGURE 15

Test #	User	Pace	Length [m] (real\est.)	Length error	Mean Pos. error
1	A	W	433\431	0.5%	1%
2	B	W	399\395	1%	2.1%
3	B	W	551\556	0.9%	0.9%
4	A	W	578\569	1.5%	1.6%
5	B	W+R	1124\1118	0.5%	1.6%
6	A	W+R	3262\3254	0.3%	1.4%

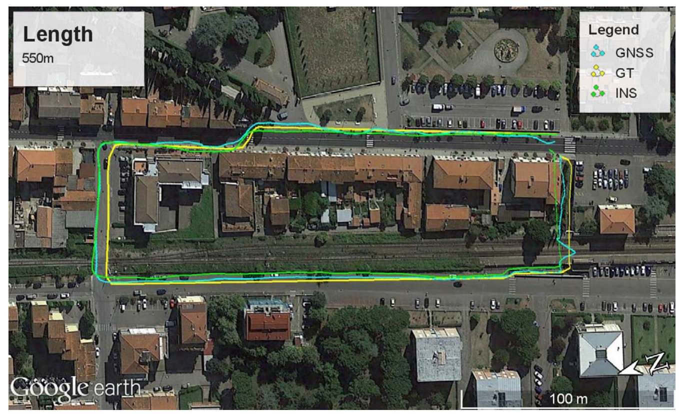

Fig. 15. Comparison between Ground-Truth (yellow), PDR/INertial-Sensors (green) and GNSS (cyan) paths in a 550 m long test characterized by straights and sharp turns (Test # 3 in Table I).

For the sake of a better understanding, during the circular trajectory the user maintains a constant velocity, so that the motion direction varies linearly, as highlighted by the green line in the upper figure. The direct and average HE are reported as well in blue and red, respectively. In the central figure the differences relative to ground-truth are also shown. On the contrary Figure 12 (bottom) shows the heading of the IMU, i.e. the angle describing its orientation with respect to the North. Since there are no assumptions on the IMU position on the user body, this angle is not equal to the actual direction of motion. However, the IMU orientation with respect to the human body does not vary during the test, and so its heading changes exactly as the direction of motion does. Also note that the oscillations in the estimated directions of motion in Figure 12 (top and bottom) have very similar amplitudes, in accordance with the observation of the waist rotation during a walk.

Figure 13 illustrates a test in which the user runs on a straight line. The corresponding data shows that the proposed method returns an accurate estimation of the direction of motion even if the subject is running.

Figure 14 reports the results of a test in which the mean values of the heading estimations – either HE (blue) and A-HE (red) – differs from ground-truth (green) because of an external magnetic disturbance, which does not allow the AHRS system to correctly estimate the IMU orientation. Magnetic field disturbances may be caused by many different sources, such as electronic devices and proximity to large metal objects, and they turned out the most serious issue in the IMU sensors accuracy.

In order to test the reliability of a complete PDR system based on the presented methods for SD, SLE and A-HE, a number of complete path estimations are presented in Table I for outdoor environment. In particular, the length error appears only related to the mean error of the step length estimation but is not affected by the heading estimation accuracy, whereas the overall PDR accuracy (mean position error in Table I) has been quantified by evaluating the distance errors between the actual and the estimated paths in specific way-points (for example, at each turn and at the end) and by computing their *Integral Mean Error* normalized with respect to the total path length.

For instance, the map of test # 3 is reported in Figure 15. Here, user (B) walked along a 550 m long path (yellow) that features a number of straight parts divided by pretty sharp curves. Notably, the estimated path (green) remains within few meters from both the actual (yellow) and the GNSS estimate (cyan) paths. In particular, the GNSS system shows a large position error when the user walks along the railway underpass, whereas the PDR system is unaffected.

Finally, Figure 16 shows an application to indoor navigation with a test performed in the School of Engineering for a 180 m

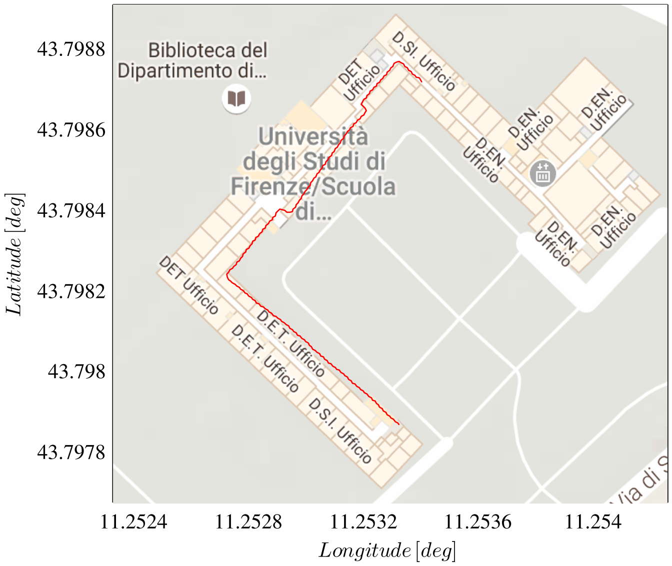

Fig. 16. Estimated path in a 180 *m* long test performed along the central corridor inside a building.

long path. The visible drift is due to a greater influence of magnetic field disturbances inside a building with respect to an outdoor environment.

V. Conclusions

In this paper a Pedestrian Dead Reckoning system has been designed to be both fairly free from the inertial sensors position on the human body, and also independent of their attitude with respect to the user. Thanks to these features the IMU device can be worn close to the lower torso area without any restriction, for instance put in a pocket or hung at the belt. Novel methods for Step Detection and Heading Estimation have been developed. The novelty in the Step Detection technique consists in the use of a Phase Locked Loop processing only vertical accelerations to match the user pace. Eventually, the innovation in the Heading Estimation method turns out in the analysis of the geometrical features of the acceleration data projected into the instant horizontal plane the user is moving onto. In this frame of reference each step corresponds to an elliptic curve whose principal axis features the acceleration/deceleration along the direction followed by that single step, while the secondary axis is related to the orthogonal motion the gait undergoes to keep the balance. These features derive from the kinematics of the waist, and they allow one to estimate the right direction through the orientation of those ellipses during a complete stride. A number of experiments have been reported to illustrate the good accuracy of the complete Pedestrian Dead Reckoning system. Future research will focus on investigating the results obtained by wearing the IMU in different positions, such as on the arm or in a bag, in order to refine the algorithm and to reduce the error in these cases through an extended body kinematics model. Moreover, new tests will be carried out to size the estimation error due to variation of the IMU attitude during the motion, such as the one related to answering a phone call while walking. Even if from very preliminary tests the algorithm is expected to be pretty insensitive of this event, a further analysis will be performed to increase the method reliability.

References

[1] L. Ojeda and J. Borenstein, "Non-gps navigation for security personnel and first responders," *J. Navigat.*, vol. 60, no. 3, pp. 391–407, Sep. 2007.

[2] X. Yun, E. R. Bachmann, H. Moore, and J. Calusdian, "Self-contained position tracking of human movement using small inertial/magnetic sensor modules," in *Proc. IEEE Int. Conf. Robot. Autom.*, Apr. 2007, pp. 2526–2533.

[3] A. R. Jimenez, F. Seco, C. Prieto, and J. Guevara, "A comparison of pedestrian dead-reckoning algorithms using a low-cost MEMS IMU," in *Proc. IEEE Int. Symp. Intell. Signal Process. (WISP)*, Aug. 2009, pp. 37–42.

[4] Y. Jin, H.-S. Toh, W.-S. Soh, and W.-C. Wong, "A robust dead-reckoning pedestrian tracking system with low cost sensors," in *Proc. IEEE Int. Conf. Pervasive Comput. Commun. (PerCom)*, Mar. 2011, pp. 222–230.

[5] S. H. Shin, C. G. Park, J. W. Kim, H. S. Hong, and J. M. Lee, "Adaptive step length estimation algorithm using low-cost MEMS inertial sensors," in *Proc. IEEE Sensors Appl. Symp. (SAS)*, Feb. 2007, pp. 1–5.

[6] H. Zhang, W. Yuan, Q. Shen, T. Li, and H. Chang, "A handheld inertial pedestrian navigation system with accurate step modes and device poses recognition," *IEEE Sensors J.*, vol. 15, no. 3, pp. 1421–1429, Mar. 2015.

[7] L.-T. Hsu, Y. Gu, Y. Huang, and S. Kamijo, "Urban pedestrian navigation using smartphone-based dead reckoning and 3-D map-aided GNSS," *IEEE Sensors J.*, vol. 16, no. 5, pp. 1281–1293, Mar. 2016.

[8] Q. Tian, Z. Salcic, K. Wang, and Y. Pan, "A multi-mode dead reckoning system for pedestrian tracking using smartphones," *IEEE Sensors J.*, vol. 16, no. 7, pp. 2079–2093, Apr. 2016.

[9] W. Kang and Y. Han, "SmartPDR: Smartphone-based pedestrian dead reckoning for indoor localization," *IEEE Sensors J.*, vol. 15, no. 5, pp. 2906–2916, May 2015.

[10] R. Feliz, E. Zalama and J. Gómez García-Bermejo, "Pedestrian tracking using inertial sensors," *J. Phys. Agents*, vol. 3, no. 1, pp. 35–43, Jan. 2009.

[11] Z.-A. Deng, G. Wang, Y. Hu, and D. Wu, "Heading estimation for indoor pedestrian navigation using a smartphone in the pocket," *Sensors*, vol. 15, no. 9, pp. 21518–21536, 2015.

[12] M. Galanti and D. Miceli, "Design of a novel IMU-based pedestrian dead reckoning system for indoor and outdoor application," M.S. thesis, Dept. Inf. Eng., Univ. Florence, Florence, Italy, Apr. 2015.

[13] S. Y. Cho, C. G. Park, and G. I. Jee, "Measurement system of walking distance using low-cost accelerometers," in *Proc. 4th ASCC*, 2002, pp. 1799–1803.

[14] S. Beauregard, "Omnidirectional pedestrian navigation for first responders," in *Proc. 4th Workshop Positioning, Navigat. Commun. (WPNC)*, Mar. 2007, pp. 33–36.

[15] I. Skog, J.-O. Nilsson, and P. Handel, "Pedestrian tracking using an IMU array," in *Proc. IEEE Int. Conf. Electron., Comput. Commun. Technol. (CONECCT)*, Jan. 2014, pp. 1–4.

[16] N. Zhao, "Full-featured pedometer design realized with 3-axis digital accelerometer," Analog Dialogue, vol. 44, no. 2, pp. 17–21, Jun. 2010.

[17] Q. Ladetto, "On foot navigation: Continuous step calibration using both complementary recursive prediction and adaptive Kalman filtering," in *Proc. ION GPS*, Salt Lake City, UT, USA, Sep. 2000, pp. 1735–1740.

[18] H. Weinberg, "Using the ADXL202 in pedometer and personal navigation applications," Analog Devices, Norwood, MA, USA, Appl. Note AN-602, 2002.

[19] P. E. Q. Garcia and W. Li, "On indoor positioning for mobile devices," M.S. thesis, Dept. Commun. Eng., Integr. Electron. Syst. Design, Chalmers Univ. Technol., Göteborg, Sweden, 2011.

[20] W. Kang, S. Nam, Y. Han, and S. Lee, "Improved heading estimation for smartphone-based indoor positioning systems," in *Proc. IEEE 23rd Int. Symp. Pers. Indoor Mobile Radio Commun. (PIMRC)*, Sep. 2012, pp. 2449–2453.

[21] U. Steinhoff and B. Schiele, "Dead reckoning from the pocket—An experimental study," in *Proc. IEEE Int. Conf. Pervas. Comput. Commun. (PerCom)*, Mar. 2010, pp. 162–170.

[22] K. Kunze, P. Lukowicz, K. Partridge, and B. Begole, "Which way am i facing: Inferring horizontal device orientation from an accelerometer signal," in *Proc. Int. Symp. Wearable Comput. (ISWC)*, Sep. 2009, pp. 149–150.

[23] F. Ichikawa, J. Chipchase, and R. Grignani, "Where's the phone? A study of mobile phone location in public spaces," in *Proc. 2nd Int. Conf. Mobile Technol., Appl. Syst.*, Nov. 2005, pp. 1–8.

[24] S. H. Pourtakdoust and H. Ghanbarpour Asl, "An adaptive unscented Kalman filter for quaternion-based orientation estimation in low-cost AHRS," *Aircraft Eng. Aerosp. Technol.*, vol. 79, no. 5, pp. 485–493, 2007.

[25] R. E. Best, *Phase-Locked Loops: Design, Simulation, and Applications*, 6th ed. New York, NY, USA: McGraw-Hill, 2007.

[26] *iNEMO Engine Pro Sensor Fusion Algorithm and API for Android-Based ARM Platforms*, STMicroelectronics, Geneva, Switzerland, 2011.

[27] *MTi-G User Manual and Technical Documentation*, Xsens Technol. B.V., Enschede, The Netherlands, 2010.

Michele Basso received the master's degree in electronic engineering from the University of Florence, Italy, in 1992, and the Ph.D. degree in systems engineering from the University of Bologna, Italy, in 1997. From 1998 to 2010, he was an Assistant Professor with the Dipartimento di Sistemi e Informatica, University of Florence. He is currently an Associate Professor with the Dipartimento di Ingegneria dell'Informazione, University of Florence. He is also with the Center for Research on Complex Dynamics and a member of the Advisory Board of the Italian Ph.D. School of Information Engineering. He was an Associate Editor of the journal *Communications in Nonlinear Science and Numerical Simulations* from 2010 to 2014. His current research interests include nonlinear dynamical systems, scanning probe microscopy, and control education.

Matteo Galanti received the bachelor's degree in electronic and telecommunications engineering and the master's degree in electrical and automation engineering from the University of Florence, Italy, in 2012 and 2015, respectively, where he is currently pursuing the Ph.D. degree in automation, optimization and complex systems with the Department of Information Engineering. His research interests include analysis of complex systems, MEMS sensors, sensor networks, and data fusion.

Giacomo Innocenti received the degree in computer science and the Ph.D. degree in nonlinear dynamics from the Engineering School, University of Florence, Italy, in 2004 and 2008, respectively. He has been a Post-Doctoral Research Fellow and an Adjunct Lecturer with the University of Florence and the University of Siena. Since 2012, he has been an Assistant Professor of Automatic Controls with the University of Florence, where he teaches industrial automation to graduate students of the Engineering School. His scientific interests regard nonlinear control systems theory and applications, and nonlinear modeling.

Davide Miceli received the bachelor's degree in electronic and telecommunications engineering and the master's degree in electrical and automation engineering from the University of Florence, Italy, in 2012 and 2015, respectively. He is currently an Innovation Engineer with Comau, Turin, Italy, where he also attends a second-level master program in industrial engineering in partnership with the Polytechnic of Turin. His research interests include inertial navigation systems, data mining, sensor fusion, and machine learning.